

Potent $\alpha 4\beta 1$ Peptide Antagonists as Potential Anti-Inflammatory Agents

David Y. Jackson,^{*,†} Clifford Quan,[†] Dean R. Artis,[†] Thomas Rawson,[†] Brent Blackburn,[†] Martin Struble,[†] Geraldine Fitzgerald,[†] Kathryn Chan,[†] Sheldon Mullins,[†] J. P. Burnier,[†] Wayne J. Fairbrother,[‡] Kevin Clark,[§] Maureen Berisini,[§] Henry Chui,^{||} Mark Renz,^{||} Susan Jones,^{||} and Sherman Fong^{||}

Departments of Bioorganic Chemistry, Immunology, Protein Engineering, and Analytical Methods Development, Genentech Inc., 460 Point San Bruno Boulevard, South San Francisco, California 94080

Received March 17, 1997[©]

The migration, adhesion, and subsequent extravasation of leukocytes into inflamed tissues contribute to the pathogenesis of a variety of inflammatory diseases including asthma, rheumatoid arthritis, inflammatory bowel disease, and multiple sclerosis. The integrin adhesion receptor $\alpha 4\beta 1$ expressed on leukocytes binds to the extracellular matrix protein fibronectin and to the cytokine inducible vascular cell adhesion molecule-1 (VCAM-1) at inflamed sites. Binding of $\alpha 4\beta 1$ to VCAM-1 initiates firm adhesion of the leukocyte to the vascular endothelium followed by extravasation into the tissue. Monoclonal antibodies generated against either $\alpha 4\beta 1$ or VCAM-1 can moderate this inflammatory response in a variety of animal models. Recently peptides containing a consensus LDV sequence based on the connecting segment-1 (CS-1) of fibronectin and cyclic peptides containing an RCD motif have shown promise in modulating leukocyte migration and inflammation presumably by blocking the interaction of $\alpha 4\beta 1$ with VCAM-1. Here we describe novel, highly potent, cyclic peptides that competitively inhibit $\alpha 4\beta 1$ binding to VCAM-1 and fibronectin at sub nanomolar concentrations. The structure of a representative analog was determined via NMR spectroscopy and used to facilitate optimization of peptide leads. The peptides discussed here utilize similar functional groups as the binding epitope of VCAM-1, inhibit lymphocyte migration *in vivo*, and are highly selective for $\alpha 4\beta 1$. Furthermore the structure–activity relationships described here have provided a template for the structure-based design of small molecule antagonists of $\alpha 4\beta 1$ -mediated cell adhesion processes.

Introduction

The integrins are α/β -heterodimeric cell surface receptors involved in numerous cellular processes from cell adhesion to gene regulation.^{1,2} Several different integrins have been implicated in disease processes and have generated widespread interest as potential targets for drug discovery.³ In the immune system, integrins are involved in leukocyte trafficking, adhesion, and infiltration during inflammatory processes.⁴ Differential expression of integrins regulates the adhesive properties of leukocytes, and different leukocytes are involved in different inflammatory responses.⁵ The integrin $\alpha 4\beta 1$ is expressed primarily on monocytes, lymphocytes, eosinophils, basophils, and macrophages but not on neutrophils.⁶ The primary ligands for $\alpha 4\beta 1$ are the endothelial surface protein vascular cell adhesion molecule-1 (VCAM-1) and the extracellular matrix protein fibronectin.⁷ The binding of the $\alpha 4\beta 1$ receptor to cytokine-induced VCAM-1 expressed on high-endothelial venules (HEVs) at sites of inflammation results in firm adhesion of the leukocyte to the vascular endothelium followed by extravasation into the inflamed tissue.⁸ Binding of $\alpha 4\beta 1$ to VCAM-1 also plays a key role in stem cell adhesion to bone marrow stromal cells⁹ and may also be involved in tumor cell metastasis.¹⁰ Monoclonal antibodies directed against $\alpha 4\beta 1$ or VCAM-1 have been shown to be effective modulators in animal models of chronic inflammatory diseases such as asthma,¹¹ rheumatoid arthritis (RA),¹² and inflamma-

tory bowel disease (IBD).^{13,14} These antibodies have also been shown to peripheralize hemopoietic progenitors in primates.^{15,16} Small molecule antagonists of $\alpha 4\beta 1$ /VCAM-1 might therefore be useful for treatment of chronic inflammatory diseases, be useful for mobilization of bone marrow stem cells, or even find utility as antitumor agents.

Recently cyclic peptide antagonists of GPIIb/IIIa/fibrinogen based on an RGD motif common in many integrin ligands have been reported.¹⁷ These cyclic peptides led to the structure-based design of novel peptidomimetic antagonists that inhibit platelet aggregation and may be useful for treatment of heart disease.¹⁸ Subsequently, cyclic peptide inhibitors containing RCD or LDV sequences were shown to block $\alpha 4\beta 1$ and $\alpha 5\beta 1$ binding to fibronectin at low micromolar concentrations.¹⁹ Indeed, many integrin ligands display similar sequences in their binding sites including fibrinogen (binds $\alpha \text{IIb}\beta \text{IIIa}$),²⁰ vitronectin (binds $\alpha \text{v}\beta 3$),²¹ and collagen (binds $\alpha 2\beta 1$),²² and compounds containing such motifs will likely become useful therapeutic agents.

The integrin-binding sites of VCAM are thought to reside in the first and fourth domains of the seven-domain protein.²³ The crystal structure of domains 1 and 2 of VCAM, solved by two independent groups,^{24,25} reveals an immunoglobulin-like fold which had been previously predicted based on sequence homology with the IgG CH1 domain and molecular modeling.²⁶ The proposed VCAM-1 integrin-binding epitope, which contains the sequence R₃₆TQID₄₀SPLN₄₄ in a surface-exposed loop connecting two β -strands (the CD-loop), suggested Arg36 and Asp40 as potentially important binding residues. Mutation of either residue to alanine in a VCAM-1/IgG chimera resulted in decreased binding affinity for cells expressing $\alpha 4\beta 1$.²⁶ We have recently

* Author to whom correspondence should be addressed.

[†] Department of Bioorganic Chemistry.

[‡] Department of Protein Engineering.

[§] Department of Analytical Methods Development.

^{||} Department of Immunology.

[©] Abstract published in *Advance ACS Abstracts*, September 1, 1997.

reported the design of cyclic amide $\alpha 4\beta 1$ peptide inhibitors (IC_{50} s in the low micromolar range) based on the VCAM CD-loop sequence TQIDSP.²⁷ The structures of these peptides were found to mimic that of the VCAM-1 CD-loop via NMR spectroscopy. In addition, amino acid substitutions in the peptides produced changes in affinity which paralleled the structure-activity relationship (SAR) of existing protein mutagenesis studies and were predictive of the activities of new mutant proteins.²⁷

The dissociation constants of ligand/integrin interactions in solution are typically weak, ranging from high micromolar to high nanomolar.^{1,2} The additivity of the multiple adhesive interactions at a cell surface (avidity), however, provides the necessary binding energy to anchor leukocytes to the vascular endothelium. We hypothesized that a therapeutically useful $\alpha 4\beta 1$ antagonist would need to have substantially higher affinity for the integrin receptor than its native protein ligands in order to block a high percentage of the cell surface interactions involved in cell adhesion. Clearly, different integrins can selectively bind a variety of ligands in solution, as part of a matrix or attached to a cell surface,^{1,2} and peptide inhibitors with different structures can selectively bind to different integrins.^{17,19} These observations led us to speculate that epitope conformation may be more important for binding selectivity than for high affinity.²⁸⁻³⁰ With this in mind, we set out to find novel $\alpha 4\beta 1$ selective antagonists which also possess the necessary affinity for *in vivo* inhibition of leukocyte adhesion and infiltration.

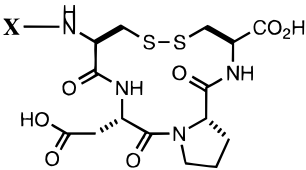
Results and Discussion

(X)CDPC Peptides. In order to more clearly define the functional binding moieties of RCD peptide inhibitors for $\alpha 4\beta 1$, we made a series of peptide analogs based on the previously described $\beta 1$ selective peptide antagonist *cyclo*-RCD(thioP)C which, when immobilized to an affinity column, bound $\alpha 4\beta 1$ and $\alpha 5\beta 1$.^{19,30} As a primary assay we measured the IC_{50} for inhibition of purified $\alpha 4\beta 1$ binding to immobilized VCAM-1 in a 96-well ELISA format (see Experimental Methods). As a secondary assay, we measured the IC_{50} for inhibition of fluorescently labeled $\alpha 4\beta 1$ positive Ramos cells binding to immobilized VCAM-1 (see Experimental Methods). The higher IC_{50} s generally observed in this cell-based assay relative to the primary assay probably result from the large number of receptors on a cell surface (> 10 000/cell)²⁶ that must be blocked in order to inhibit cell adhesion.

Our first set of analogs were designed to assess the effect of N-terminal substitution in the cyclic pentapeptide RCDPC (**1**) which has an IC_{50} of 3.7 μM by protein-based ELISA (Table 1). Previous mutagenesis studies of VCAM-1 showed that mutation of Arg36 to Ala resulted in decreased binding affinity, implicating Arg36 as an important contact residue.²⁶ If the *cyclo*-RCDPC peptide (**1**) mimics the VCAM-binding epitope for $\alpha 4\beta 1$, then Arg substitution in the peptide should result in an analogous loss of affinity. Accordingly, substitution of Lys for Arg (**3**) resulted in decreased binding affinity (Table 1).

Acylation of the N-terminal Arg of *cyclo*-RCD(thioP)C with hydrophobic groups had previously been shown to enhance binding affinity.^{19,30} We found that N-terminal

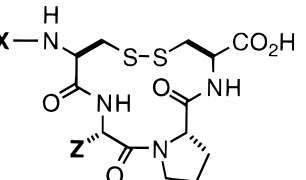
Table 1. Inhibition of $\alpha 4\beta 1$ /VCAM-1 by (X)CDPC Peptides



X-CDPC core structure

no.	X	IC_{50} (μM)	
		ELISA	Ramos
1	Arg	3.7	80
2	Ac-Arg	1.3	40
3	Lys	~250	~1000
4	Fmoc-Arg	0.13	15
5	Leu-Arg	21.0	250
6	Phe-Arg	2.1	100
7	Trp-Arg	1.2	100
8	Tyr-Arg	0.11	6
9	Tyr-Lys	0.15	5
10	Tyr-Ala	0.21	5
11	Tyr	0.004	0.4

Table 2. Inhibition of $\alpha 4\beta 1$ /VCAM-1 by XC(Z)PC Peptides



XC(Z)PC core structure

no.	X	Z	IC_{50} (μM)	
			ELISA	Ramos
8	Tyr-Arg	Asp	0.11	6.0
12	Tyr-Arg	Glu	0.09	30
13	Tyr-Arg	Asn	0.04	7.0
14	Tyr-Arg	Gln	0.05	9.0
15	Tyr-Arg	Ala	0.06	8.0
16	Ac-Tyr	Asp	0.003	0.30
17	Ac-Tyr	Ser	0.002	0.12
18	Ac-Tyr	Thr	0.005	0.32
19	Ac-Tyr	Tyr	0.003	0.23
20	Ac-Tyr	Ala	0.004	0.31

extension of *cyclo*-RCDPC (**1**) with the hydrophobic residues Leu, Phe, and Trp (**5-7**) had little effect on binding affinity (Table 1). However, aminoacylation of Arg with Tyr (**8**) resulted in a substantial improvement in affinity ($IC_{50} = 0.11 \mu M$). The Tyr hydroxyl appears to contribute the majority of this affinity enhancement because the corresponding Phe analog (**6**) had reduced affinity. Surprisingly, substitution of Arg in YRCDPC (**8**) with Lys (**9**) or Ala (**10**) resulted in little change in affinity. In fact deletion of Arg to afford **11** led to further improvement of affinity ($IC_{50} = 4 \text{ nM}$) indicating that Arg in these peptides is neither an essential nor optimal residue in the binding of these molecules to $\alpha 4\beta 1$. Because **11** also inhibits binding of a competitive $\alpha 4$ specific monoclonal antibody but does not inhibit a competitive VCAM-1 specific antibody from binding to VCAM (data not shown), it is likely that inhibition is due to selective binding of **11** to $\alpha 4\beta 1$ but not VCAM-1. Overall, the simple substitution of Arg to Tyr (**11**) in the parent RCDPC cyclic peptide **1** enhanced the binding affinity for $\alpha 4\beta 1$ by nearly 1000-fold.

XC(Z)PC Peptides. In addition to Arg, Asp has also been implicated as an important residue for $\alpha 4\beta 1$ -mediated cell adhesion to fibronectin and VCAM-1. Mutation of Asp40 in VCAM-1 to Ala virtually elimi-

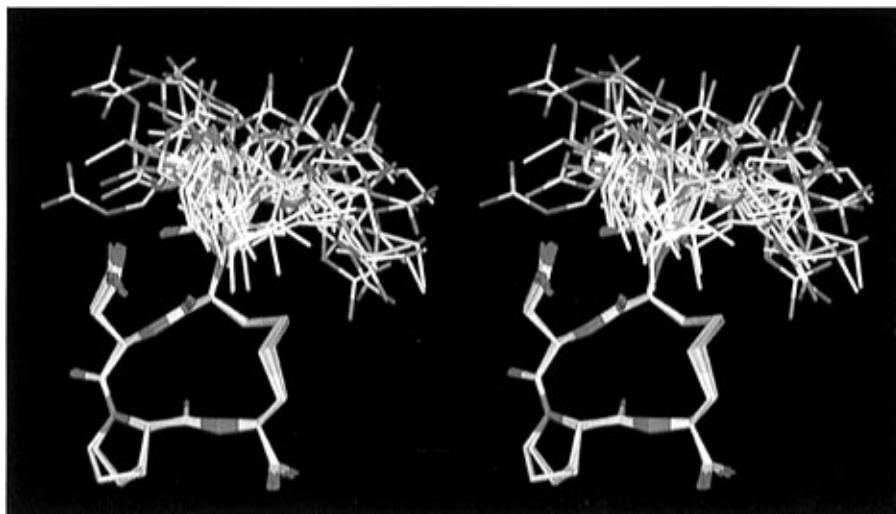


Figure 1. Representative low-energy structures (stereo) from the NMR ensemble of **5**.

nated binding to $\alpha 4\beta 1$.²⁶ In addition, substitution of Asp in RCD peptides¹⁹ or in fibronectin CS-1-based peptide inhibitors containing a consensus LDV motif³¹ abolished activity of the peptides. Using the cyclic peptides YRCDPC (**8**) or Ac-YCDPC (**16**) as references, analogs were made to assess the importance of aspartic acid in these peptide inhibitors. From the data shown in Table 2, it is apparent that a wide variety of substitutions are permitted at this position with little effect on binding affinity. This strongly suggests that the cyclic peptides do not bind in the same orientation as the native protein ligands. On the basis of the data presented thus far, we conclude that RCD is sufficient for inhibitory activity but neither Arg nor Asp is essential or optimal for potent inhibition of $\alpha 4\beta 1$ binding to VCAM-1. Because the effects of Arg or Asp substitution in **8** on inhibition of $\alpha 4\beta 1$ /fibronectin are similar (data not shown), the peptides probably bind the $\alpha 4\beta 1$ receptor but do not bind its ligands VCAM-1 or fibronectin.

NMR Structural Analysis. In order to investigate possible structural similarities between the cyclic peptides and the VCAM-1 CD-loop, we determined the structure of a representative peptide (LRCDPC, **5**) via NMR spectroscopy (Figure 1). The final set of refined structures contains no distance restraint violations $> 0.07 \text{ \AA}$ and no dihedral restraint violations $> 3.4^\circ$. The cyclic CDPC core of **5** was found to adopt a well-ordered structure in solution dominated by a distinct conformation. In contrast the N-terminal Leu-Arg residues are highly disordered. The constraint imposed by the disulfide bond was found to fold the peptide into a very tight turn marked by a *cis*-amide bond at the Asp-Pro linkage. Interestingly, analysis of coupling constant and NOE data indicated that the χ_1 of the Asp side chain was constrained to values of $\sim -60^\circ$. While the apparent disorder of the N-terminal residues would appear to limit the role Arg might be playing in this conformation, an Arg-Asp salt bridge appears possible and may be one of the factors contributing to the limited rotation at the Asp χ_1 , as some of the structures consistent with the NMR restraints exhibit this feature. The lack of structural similarity between peptide **5** and the VCAM-1 CD-loop (discussed later), and the fact that neither Arg nor Asp is essential for peptide binding to $\alpha 4\beta 1$, led us to conclude that the peptides are not straightforward mimics of VCAM-1. These observations coupled with

Table 3. Inhibition of $\alpha 4\beta 1$ /VCAM-1 by Cyclic XCA(Z)C Peptides

XCA(Z)C core structure

no.	X	Z	IC ₅₀ (μM)	
			ELISA	Ramos
20	Ac-Tyr	Pro	0.004	0.31
21	Ac-Tyr	Gly	22.0	ND
22	Ac-Tyr	<i>N</i> -methylglycine	0.71	ND
23	Ac-Tyr	Pip	0.001	0.02
24	Ac-Tyr	phenyl-Gly	0.076	33
25	Tyr	Pro	0.005	0.12
26	Tyr	Ile	0.023	0.94
27	Tyr	Leu	0.034	10.5
28	Tyr	Phe	2.80	182
29	Tyr	Oic	0.02	4.7
30	Tyr	γ -hydroxy-Pro	0.005	ND
31	Tyr	<i>O</i> -benzyl- γ -hydroxy-Pro	0.04	ND
32	Tyr	cyclohexyl-Ala	0.14	25
33	Tyr	cyclohexyl-Gly	0.23	ND
34	Tyr	2-aminoindane-2-carboxylate	36.0	ND

the importance of the N-terminal Tyr of **11** (which is not present in the CD-loop) led us to hypothesize that the cyclic peptides might bind $\alpha 4\beta 1$ in a different orientation or at a different site relative to the VCAM-1 CD-loop.

XCA(Z)C Analogs. Pro42 was previously found to be an important binding determinant of the VCAM-1 CD loop.²⁶ The peptides *cyclo*-Ac-YCAPC (**20**) and *cyclo*-YCAPC (**25**) were chosen as references for evaluating the importance of proline within the cyclic peptide core (Table 3). The large increase in IC₅₀ (~ 5000 -fold) upon substitution of proline (**20**) with glycine (**21**) demonstrates that proline also plays a significant role in the interaction of these cyclic peptides with $\alpha 4\beta 1$ (Table 3). Because proline often plays a unique conformational role in protein and peptide backbone structure, it is possible that the loss of affinity upon proline substitution is due to a conformational change in the CAPC core as well as loss of a potential hydrophobic interaction. Consistent with this notion, substitution of Pro with *N*-methylglycine (**22**) only partially restored affinity relative to **21**

Table 4. Effect of C-Terminal Carboxylic Acid Substitutions

no.	sequence	IC ₅₀ (μM) ^a	OH/NH ₂
1	RCDPC-acid	4.0	
35	RCDPC-amide	50.0	12.5
36	1-FCA-RCDPC-acid	0.04	
37	1-FCA-RCDPC-amide	0.30	7.5
38	YC(<i>m</i> -aminobenzoyl)C-acid	0.008	
39	YC(<i>m</i> -aminobenzoyl)C-amide	12.0	1500
20	Ac-YCAPC-acid	0.003	
40	Ac-YCAPC-amide	0.320	107

^a IC₅₀s are from the protein ELISA.

and substitution of Pro in **25** with Ile (**26**) and Leu (**27**) resulted in slight decreases in affinity.

Substitution with L-pipecolic acid (Pip) to afford **23** actually improved affinity in both protein- and cell-based assays and was the only Pro substitution which did not adversely affect activity (Table 3). Notably, substitution with Phe (**28**) resulted in a dramatic decrease in affinity. Constraint of the Phe side chain via substitution by 2-aminoindane-2-carboxylate (**34**) increased the IC₅₀ an additional 10-fold. Extension of Pro to the bicyclic octahydroindolecarboxylate (Oic) (**29**) produced a modest increase in the IC₅₀. This was increased a further 7-fold by substitution of cyclohexyl-Ala (**32**), indicating some measure of the value of the side chain constraint for this system. Substitution of γ -hydroxyproline for proline (**30**) resulted in virtually no change in IC₅₀, and the *O*-benzyl analog (**31**) of this compound showed a modest 8-fold decrease in affinity, indicating the putative site for the proline had neither a strict hydrophobic requirement nor a completely restrictive steric boundary.

These results led us to speculate that the proline might be interacting with a region of relatively open hydrophobic surface, possibly by stacking against a delocalized π -system on the receptor. The surprising decrease in affinity (20-fold) between the largely isosteric cyclohexyl-Ala (**32**) and Phe (**28**) residues suggested the latter might be positioned such that the interaction between π -systems was repulsive. Modeling studies based on the core residues from the NMR structure determined above suggested an acceptable repositioning of the aromatic ring could be achieved using phenylglycine (**24**). This substitution provided a compound which exhibited a 40-fold improvement over the phenylalanine analog **28** and was 3-fold better than the corresponding cyclohexylglycine-containing peptide **33**.

C-Terminal Carboxylate Substitutions. Asp40 of VCAM-1 was previously shown to be an important integrin-binding residue as determined by alanine scanning mutagenesis,²⁶ yet Asp is not an essential residue in the cyclic peptides discussed here (see Table 2). Because the importance of proline in both peptide and protein binding was well established and the link between protein and peptide SAR suggested they bind an overlapping site on the receptor, we hypothesized that the C-terminal carboxylate in the peptides might occupy a site on the receptor normally filled by Asp40 of VCAM-1. To test this hypothesis we prepared several C-terminal carboxamide analogs and compared them with the corresponding C-terminal acids (Table 4). Notably, C-terminal carboxamide substitution in peptides containing Asp (**1**, **35–37**) resulted in a moderate (~10-fold) reduction in binding affinity, while a much

more dramatic (100–1500-fold) effect was seen for peptides lacking aspartic acid (**20**, **38–40**). These results demonstrate that the C-terminal carboxylate group of RCXPC-like peptides is an important binding determinant, and the loss of affinity upon carboxamide substitution can be partially recovered if Asp is present at the X position. Accordingly, Asp substitution in the native protein ligands²⁶ and in cyclic peptides based on the VCAM-1 CD-loop sequence *cyclo*-TQIDSPXX-amide²⁷ resulted in relatively large decreases in affinity.

The results from Table 4 have led us to hypothesize that RCDPC-like peptides containing Asp might bind in two possible orientations: one in which the conformationally rigid C-terminal carboxylate group preferentially fills a putative electrostatic Asp-binding site or a second less important orientation in which the Asp side chain fills the carboxylate-binding site similar to the native protein ligands. Peptides not containing Asp would be restricted to a single orientation utilizing the C-terminal carboxylate group resulting in a more significant decrease in binding affinity upon conversion to a carboxamide. Further studies are being conducted to test this hypothesis and more clearly define the interaction of the cyclic peptides with $\alpha4\beta1$.

Comparison of Peptide and Protein Binding Properties. Previous mutagenesis studies on VCAM-1 have implicated Arg36, Asp40, and Pro42 as important residues for binding to $\alpha4\beta1$.^{26,28} The X-ray structure of the first domain of VCAM-1 highlighting the CD-loop (depicted in white) and Arg36, Asp40, and Pro42 (depicted in green) is shown in Figure 2.²⁴ For comparison, representative structures from the NMR ensemble of **5** (from Figure 1) are also shown. Because the CD-loop of VCAM-1 is involved in crystal-packing interactions with three other molecules of the protein, the actual receptor-binding conformation of the CD-loop in VCAM-1 is likely to be different from that depicted in the X-ray structure.²⁴ We have recently designed cyclic amide peptides of the general sequence TQIDSP based on the VCAM CD-loop sequence and X-ray structure. Using NMR and binding displacement assays, we showed that these peptides mimic the VCAM CD-loop structure and bind with low micromolar affinities.²⁷ Inspection of Figure 2 led us to conclude that although the cyclic disulfide peptides described here share little sequence homology with the VCAM CD-loop region, they demonstrate some structural similarities primarily near the proline- and carboxylate-binding moieties implicating a likely overlap in binding sites. In addition, we have recently used a fluorescently labeled BCK(*N*-fluorescence)PC peptide (**77**) (ELISA IC₅₀ = 8 nM) in displacement assays to confirm that the cyclic disulfides described here can be competitively displaced from the $\alpha4\beta1$ receptor by both VCAM and the aforementioned cyclic amide CD-loop-based peptides. These results (discussed in ref 27) further support the hypothesis that all three bind a similar overlapping site on the receptor.

(X)CSPC Peptides. The data presented thus far have demonstrated that potent inhibition is achieved by the consensus sequence YCXPC with the N-terminal Tyr, the endocyclic Pro, and the C-terminal carboxylate contributing most of the binding energy. The data presented below (Table 5) show the results of a similar effort to optimize the N-terminal Tyr for stability and

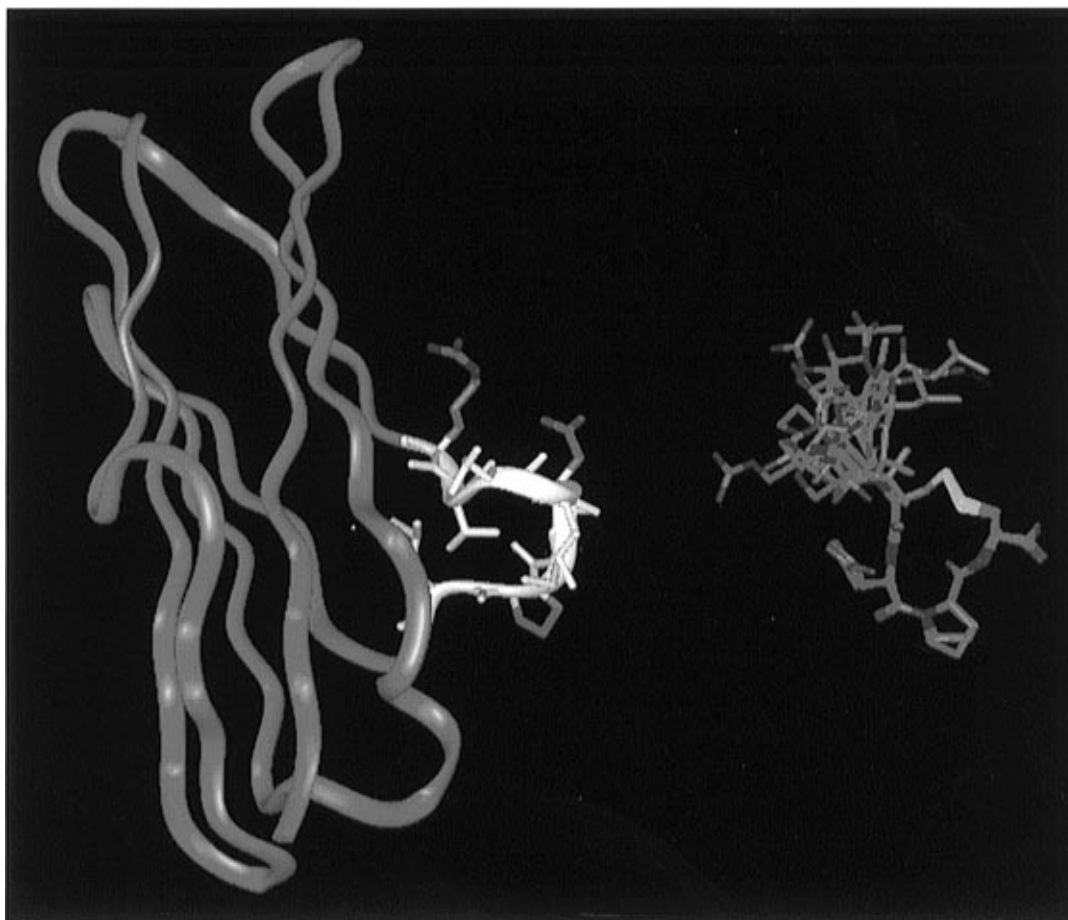


Figure 2. Comparison of the VCAM-1 X-ray structure²⁴ (left) and the NMR structure of **5** (right). The VCAM-1 CD-loop (white) with Arg36, Asp40, and Pro42 (green) is shown.

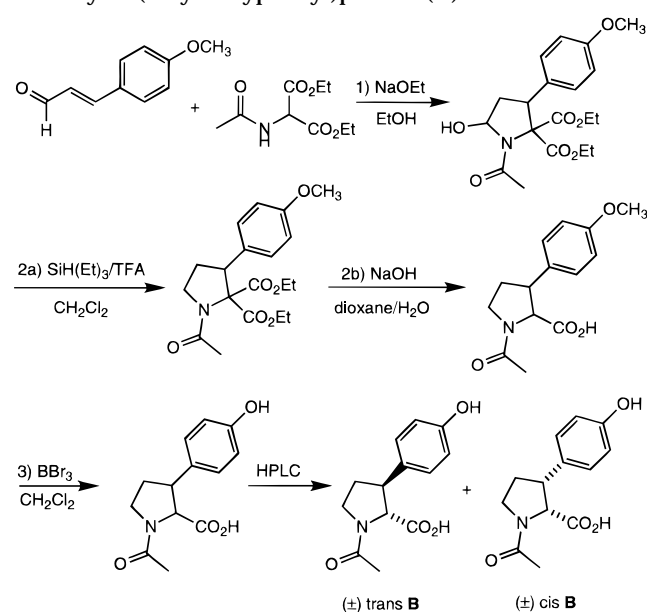
Table 5. N-Terminal Optimization of Cyclic (X)CSPC Peptides

no.	X	IC ₅₀ (μ M)	
		ELISA	Ramos
17	Ac-Tyr	0.002	0.06
41	D-Tyr	0.89	126
42	Phe	1.50	15.0
43	benzoyl	0.134	1.9
44	isonipecotyl	4.60	50
45	4-methoxyphenylacetyl	0.25	3.0
46	1-fluorenylcarboxyl	0.14	1.5
47	1-naphthoyl	0.097	6.3
48	2-naphthoyl	0.054	3.6
49	3-hydroxy-Phe	0.25	25
50	3-iodo-Tyr	0.004	0.2
51	3-fluoro-Tyr	0.008	0.5
52	3-chloro-Tyr	0.007	0.6
53	4-(4-hydroxyphenyl)benzoyl	1.65	120
54	2,3,5,6-tetrafluoro-Tyr	0.53	60
55	6-hydroxynaphthoyl	1.10	40
56	2-phenyl-3-(4-hydroxyphenyl)propionyl	0.013	2.0
57	(\pm)- <i>trans</i> - B	0.0005	0.008
58	(\pm)- <i>cis</i> - B	0.004	ND

potency. The cyclic disulfide Ac-YCSPC (**17**) was chosen as a reference compound for comparative purposes. When the hydroxyl group of Tyr was moved to the meta

position (**49**), a substantial decrease in affinity was observed. In addition, a dramatic loss of potency is seen when Tyr is replaced by Phe (**42**), demonstrating the importance of the Tyr hydroxyl for high-affinity binding. In general, other Tyr substitutions resulted in loss of affinity; however, halogen substitution ortho to the Tyr hydroxyl group (**50–52**) had a minimal effect on potency. Other phenol analogs also demonstrated decreased affinity relative to **17** highlighting the essential role of Tyr in this position. Substitution of the Tyr *N*-acetyl with a phenyl group (**56**) resulted in only a slight decrease in binding affinity consistent with the earlier observation that removal of the Tyr *N*-acetyl group (**25**, Table 3) also had little effect on binding affinity.

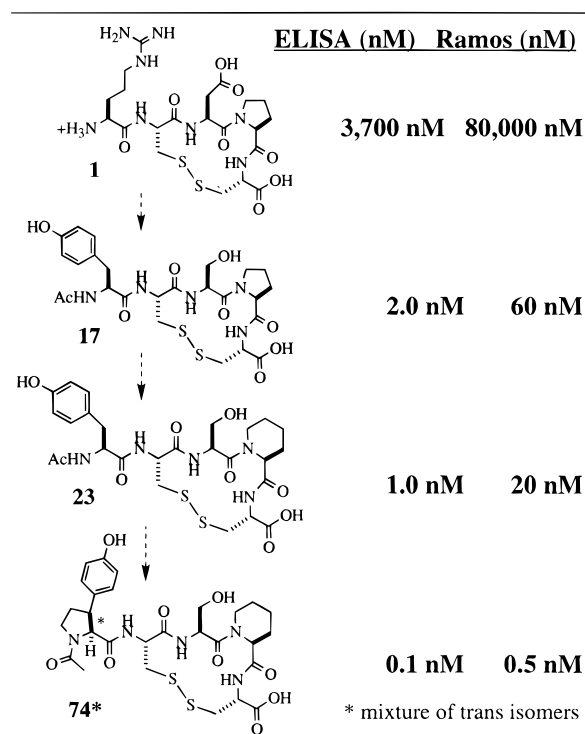
With these results in mind, we synthesized the amino acid analog **B** (Scheme 1) in which the Tyr side chain conformation is constrained by a two-carbon bridge between the β -carbon and the amino group. We hoped that the further constraint of the phenol side chain imposed in **B** would result in a favorable entropic effect on binding. The synthetic route to **B** (Scheme 1) was based on previously described 3-substituted proline derivatives.³² The amino acid analog **B** was synthesized as a mixture of *cis/trans*-isomers which could be resolved by preparative C₁₈ HPLC and incorporated into peptides to yield the corresponding peptide analogs **57** and **58** (Table 5). Analog **57**, which contains (\pm)-*trans*-**B**, showed 8-fold enhanced affinity relative to **17** in the cell-based assay, while the corresponding (\pm)-*cis*-isomer **58** had slightly reduced affinity relative to **17**. Because

Scheme 1. Synthesis of *N*-Acetyl-3-(4-hydroxyphenyl)proline (**B**)

Table 6. Inhibition of $\alpha 4\beta 1$ /VCAM-1 by Cyclic YC(X)C

no.	X	IC ₅₀ (μ M)	
		ELISA	Ramos
25	Ala-Pro	0.005	0.12
59	Pro-Ala	0.230	14.0
60	Gly	5.80	250
61	Ala	9.40	350
62	β -Ala	4.20	210
63	3-aminoisobutyryl	0.047	2.7
64	4-aminobutyryl	0.038	1.0
65	5-aminopentanoyl	0.410	17
66	isonipecotyl	0.031	1.5
67	2-aminobenzoyl	1.30	80
38	3-aminobenzoyl	0.008	0.12
68	4-aminobenzoyl	0.16	4.2
69	4-(aminomethyl)benzoyl	0.42	15
70	3-aminomethyl)benzoyl	6.00	210
71	4-(aminomethyl)cyclohexylcarbonyl	0.100	19
72	cyclohexyl-Gly	115.0	ND
73	cyclohexyl-Ala	18.00	ND

substitution of Tyr with *D*-Tyr (**41**) also resulted in a substantial loss of affinity, we hypothesized that the more active of the two *trans*-diastereomers present in **57** probably has an *L*-configuration at the α -carbon.

YC(X)C Peptides. With the relative individual contributions of the Asp-Pro in RCDPC being well established (Tables 2 and 3), analogs were designed to probe the possibility of replacing both residues simultaneously with natural or synthetic amino acids. Our goal was to reduce the cyclic peptides to a minimal high-affinity inhibitor. As a reference compound for comparative purposes we chose YCAPC (**25**) (Table 6). Significantly, compound **59** in which Ala and Pro were swapped demonstrates the necessity of Pro being in the correct position. Other substitutions in which backbone length and side chains were varied generally yielded less active compounds (Table 6). An optimal backbone


Figure 3. Additivity of functional group optimizations at the Arg, Asp, and Pro positions of the lead peptide RCDPC (**1**).

length of five atoms between the two cystines was determined based on data for the simple carbon analogs **60**, **62**, **64**, and **65**. The 3-aminobenzoyl analog **38**, which is also a five-atom linker, shows that aromatic substitutions are well tolerated without significant loss of activity. Overall the peptide backbone bridging the two cystines appears to contribute substantially to the activity of the cyclic peptides: with length, conformation, and hydrophobicity all being important factors.

Additivity of Optimizations. In an effort to further enhance the potency of this class of cyclic peptides, optimizations at the N-terminus and the endocyclic proline were combined (Figure 3). The effects of N-terminal substitution with (\pm)-*trans*-**B** (**57**) and Pro substitution with the six-membered pipecolic acid (Pip) analog **23** were essentially additive yielding **74** which demonstrated subnanomolar potency in both the protein- and cell-based assays (Figure 3). Overall, **74** was approximately 10^6 times more potent than the original RCDPC lead peptide (**1**)¹⁹ and over 500 times more potent than the native $\alpha 4\beta 1$ ligand VCAM (ELISA IC₅₀ \sim 50 nM). These results further demonstrate that although Arg and Asp motifs may be functionally important epitopes in the native $\alpha 4\beta 1$ ligands VCAM-1 and fibronectin, they are not optimal for high-affinity binding of RCDPC-like cyclic peptides to the $\alpha 4\beta 1$ integrin receptor.

Selectivity for $\alpha 4\beta 1$. The previously reported peptide RCD(thioP)C was shown to bind both $\alpha 4\beta 1$ and $\alpha 5\beta 1$ suggesting selectivity for $\beta 1$ integrins.¹⁹ We tested the cyclic peptide **17** (Ac-YCSPC) in two other previously described *in vitro* ELISA assays including fibronectin/ $\alpha 5\beta 1$ ³⁴ and fibrinogen/IIBIIa.¹⁷ Compound **17** did not inhibit fibrinogen binding to GPIIbIIIa at concentrations up to 500 μ M. Inhibition of fibronectin binding to $\alpha 5\beta 1$ was observed with **17** (IC₅₀ = 2.5 μ M) which probably reflects the binding component of **17** for the $\beta 1$ -subunit.

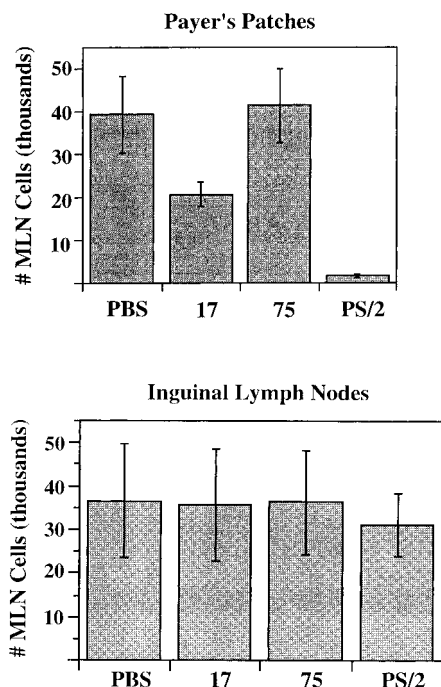


Figure 4. Inhibition of lymphocyte homing by **17** versus the known $\alpha 4$ specific antibody (PS/2)²⁶ and the negative control peptide YASPA (**75**).

Although **17** does inhibit $\alpha 5\beta 1$ /fibronectin, it is over 1000 times more potent as an inhibitor of $\alpha 4\beta 1$ /VCAM (IC₅₀ = 2 nM) demonstrating a remarkable selectivity of this peptide for $\alpha 4\beta 1$. Highly selective antagonists are desirable to maximize anti-inflammatory activity while minimizing potential side effects due to unwanted inhibition of other protein interactions.

In Vivo Lymphocyte Homing Activity. Lymphocyte homing to Peyer's patch high-endothelial venules (HEVs) is known to be dependent upon the interaction of cell adhesion molecules expressed on HEVs and $\alpha 4$ integrins expressed on lymphocytes.^{5,33,35} The accumulation of radiolabeled lymphocytes in Peyer's patches can be inhibited by treatment with anti- $\alpha 4$ antibodies.³⁶ In order to assess the activity of a representative cyclic peptide *in vivo*, mice were treated intravenously with analog **17** (0.5 mg/mouse) prior to injection with ⁵¹Cr-labeled mesenteric lymph node cells (see Experimental Methods). As negative controls, mice were treated with buffer or the linear peptide YASPA (**75**) which does not inhibit the $\alpha 4\beta 1$ /VCAM-1 interaction. An anti- $\alpha 4$ IgG (PS/2) was used as a positive control. The data shown in Figure 4 demonstrate that pretreatment of mice with **17** significantly inhibits lymphocyte accumulation in Peyer's patches while similar treatment with the control peptide **75** does not. Importantly, **17** did not inhibit migration to other tissues such as the inguinal lymph nodes where VCAM-1 is not expressed in high levels (Figure 4). These results suggest that peptide or small molecule antagonists similar to **17** may be useful for treating $\alpha 4\beta 1$ -associated inflammation *in vivo*.

Conclusions

We have demonstrated that cyclic peptides can competitively inhibit the interaction of the integrin $\alpha 4\beta 1$ with VCAM-1 at subnanomolar concentrations. The peptides bind $\alpha 4\beta 1$ with affinities several orders of magnitude tighter than the native protein ligands

VCAM-1 and fibronectin. These peptides share important functional groups with the first domain of VCAM-1 but show little direct structural similarity to the protein. Significantly, the peptides can inhibit lymphocyte homing *in vivo*, making them potential therapeutic agents for treatment of a variety of inflammatory diseases. Furthermore, we have used these peptides as templates for the structure-based design of potent small molecule antagonists (which are also active *in vivo*) of the VCAM/ $\alpha 4\beta 1$ interaction; reports on the design, structure, and activities of these novel small molecules are forthcoming.

From an evolutionary point of view, it is possible that selective pressure on cell adhesion molecules leads to optimization of specificity rather than affinity. The charged epitopes found in many integrin ligands may possess the necessary properties. One can imagine slight variations in conformation leading to a diverse range of integrin-binding specificities, allowing very similar adhesion molecules to recruit a variety of different inflammatory cells at different stages of inflammation. The evolution of high-affinity interactions between cell adhesion molecules and their cell surface integrin receptors may have proven undesirable by preventing mobilization or extravasation, with the leukocytes being virtually stuck to the endothelium unable to carry out their functions.

Although therapeutic strategies involving integrin antagonists are relatively new, antibodies, peptides, and small molecules that block integrin interactions are currently under clinical investigation for a variety of indications, and new strategies are constantly being proposed. Recently, Pasqualini *et al.* showed that a soluble high-affinity form of fibronectin (superfibronectin) could inhibit tumor cell metastasis presumably by blocking the interaction of $\alpha 5\beta 1$ positive tumor cells with wild-type fibronectin *in vivo*, thus expanding the potential for integrin antagonists.³⁷ The results presented here provide still further evidence that blocking integrin-mediated cell adhesion interactions, specifically $\alpha 4\beta 1$ /VCAM, may lead to new classes of small molecule anti-inflammatory agents.

Experimental Methods

Peptide Synthesis. All peptides were synthesized manually using standard solid phase peptide chemistry³⁸ with Fmoc-protected amino acids³⁹ on a *p*-alkoxybenzyl alcohol resin.⁴⁰ All amino acids were purchased from Bachem (CA), Advanced ChemTech U.S.A., or Calbiochem Corp. (CA). Couplings were performed with 2–4 equiv of HBTU-activated amino acid and 4 equiv of *N*-methylmorpholine. Fmoc groups were removed with 20% piperidine in DMA. Cleavage and deprotection with TFA containing 5% triethylsilane afforded crude linear peptides after washing the resin with diethyl ether to remove protecting groups. The crude peptides were then extracted from the resin by stirring with 100 mL of 2:1 H₂O/CH₃CN for 5 min followed by filtration. Disulfide oxidation was carried out at 25 °C via dropwise addition of a saturated solution of iodine in acetic acid to the crude extracts with vigorous stirring until a slight yellow color persisted. The crude oxidized peptides were lyophilized and purified by preparative reverse phase C₁₈ HPLC (CH₃CN/H₂O gradient, 0.1% TFA) to afford purified material. Pure fractions (>98% pure by analytical HPLC) were characterized by electrospray ionization mass spectrometry (Sciex API100) and lyophilized to dryness. The purified peptides were dissolved in DMSO at 10 mM just prior to assay. Serial dilutions of peptide starting at 0.5 mM were titrated into the ELISA assay, and the IC₅₀ for each peptide was determined.

N-Acetyl-3-(4-hydroxyphenyl)proline (B). The amino acid analog **B** (Table 5) was synthesized (see Scheme 1) using a modified procedure of Chung *et al.*³² and incorporated into peptides **57** and **58** (Table 5) as described.

(1) To a solution of diethyl acetamidomalonate (73.7 g) in 600 mL of anhydrous ethanol was added 20 mL of sodium ethoxide (1 M in ethanol), the solution was stirred at room temperature for 15 min, 4-methoxycinnamaldehyde (50 g) was added in one portion, and stirring was continued overnight. The solvent was evaporated, and the crude residue was chromatographed on silica gel (4:1 ethyl acetate/hexane). Evaporation of solvent afforded 106 g (91%) of pure diethyl 1-acetyl-5-hydroxy-3-(4-methoxyphenyl)pyrrolidine-2,2-dicarboxylate: ¹H NMR (300 MHz, CDCl₃) δ 7.11 (d, 2H, *J* = 9 Hz, aromatic H), 6.86 (d, 2H, *J* = 9 Hz, aromatic H), 4.29 (q, *J* = 7.5 Hz, 2H), 3.89 (m, 3H), 3.81 (s, 3H), 3.75 (m, 2H), 2.61 (m, 1H), 2.26 (m, 1H), 2.15 (s, 3H), 1.3 (t, *J* = 7.5 Hz, 3H), .86 (t, *J* = 7.5 Hz, 3H); HRMS calcd for C₁₉H₂₅NO₆ 363.1682, found 363.1684.

(2a) To 100 g of diethyl 1-acetyl-5-hydroxy-3-(4-methoxyphenyl)pyrrolidine-2,2-dicarboxylate (from step 1) in 500 mL of CHCl₃ was added 50 g of triethylsilane followed by 150 mL of trifluoroacetic acid dropwise. The solution was stirred overnight at room temperature and evaporated to dryness to afford 92 g of diethyl 1-acetyl-3-(4-methoxyphenyl)pyrrolidine-2,2-dicarboxylate which was used directly in the next step without further isolation or purification.

(2b) Diethyl 1-acetyl-3-(4-methoxyphenyl)pyrrolidine-2,2-dicarboxylate (90 g, from above) was dissolved in dioxane (500 mL), a solution of sodium hydroxide (30 g) in water (250 mL) was added, and the mixture was heated at reflux for 48 h. After cooling the solution was filtered and the filtrate acidified with concentrated HCl. The acidified solution was concentrated under vacuum to remove dioxane/water and resuspended in 300 mL of water. The product was extracted into ethyl acetate (3 × 300 mL), the organics were concentrated, and the product was purified on silica gel (eluted with ethyl acetate) to afford 54 g of 1-acetyl-3-(4-methoxyphenyl)pyrrolidine-2-carboxylic acid (77%, two steps) after evaporation of solvent: HRMS calcd for C₁₄H₁₇NO₄ 263.1157, found 263.1159; ¹H NMR (300 MHz, CDCl₃) δ 7.12 (d, 2H, *J* = 9 Hz, aromatic H), 6.87 (d, 2H, *J* = 9 Hz, aromatic H), 4.61 (d, 1H, *J* = 5 Hz, CH), 3.87 (m, 1H, CH), 3.79 (s, 3H, OCH₃), 3.65 (m, 2H, CH₂), 2.40 (m, 1H, CH), 2.10 (d, 3H, *J* = 9.6 Hz, acetyl), 2.03 (m, 1H, CH).

(3) 1-Acetyl-3-(4-methoxyphenyl)pyrrolidine-2-carboxylic acid (50 g, from step 2b) was dissolved in CH₂Cl₂ (700 mL) and cooled to -78 °C under N₂. Boron tribromide (1 M in CH₂Cl₂, 380 mL) was added dropwise with stirring, and the solution was allowed to warm to room temperature. Stirring was continued overnight; the reaction mixture was poured into 500 g of ice and neutralized via addition of solid sodium bicarbonate. The aqueous layer was separated and acidified with concentrated HCl. The product was extracted into ethyl acetate (3 × 300 mL) and purified on silica gel (9:1 ethyl acetate/acetic acid) to afford 41 g (87%) of *N*-acetyl-3-(4-hydroxyphenyl)proline (**B**) after evaporation of solvent. The *cis/trans*-isomers were separated by preparative C₁₈ HPLC. Ratio of isomers = 3:1 *trans/cis* by analysis: C₁₈ HPLC (25 cm × 1.5 mm, 1.5 mL/min, 20–50% CH₃CN/H₂O in 15 min) *t*_R = 7.21 min (*trans*), 7.63 min (*cis*); HRMS calcd for C₁₃H₁₅NO₄ 249.1001, found 249.1004; ¹H NMR for (±)-*trans*-**B** (300 MHz, CD₃OD) δ 7.10 (d, 2H, *J* = 8.7 Hz, aromatic), 6.75 (d, 2H, *J* = 8.7 Hz, aromatic), 4.31 (d, 1H, *J* = 6.6 Hz, CHα), 3.79 (m, 1H, CH), 3.75 (m, 1H, CH), 3.40 (m, 1H, CH), 2.35 (m, 1H, CH), 2.11 (s, 3H, acetyl), 2.08 (m, 1H, CH); ¹H NMR for (±)-*cis*-**B** (300 MHz, CD₃OD) δ 7.10 (d, 2H, *J* = 8.7 Hz, aromatic), 6.75 (d, 2H, *J* = 8.7 Hz, aromatic), 4.40 (d, 1H, *J* = 5.4 Hz, CHα), 3.79 (m, 1H, CH), 3.75 (m, 1H, CH), 3.40 (m, 1H, CH), 2.35 (m, 1H, CH), 2.11 (s, 3H, acetyl), 2.08 (m, 1H, CH). *Cis/trans* assignments were made by analogy of CHα coupling constants with *N*-acetyl-3-phenylproline from ref 32.

Synthesis of BCK(N-fluorescence thiourea)PC (77). The peptide **BCKPC** (**76**) (10 mg, ELISA IC₅₀ = 2 nM) was synthesized using standard methods as described and added to a solution of fluorescence isothiocyanate (10 mg; Sigma) in

5 mL of aqueous 4% sodium bicarbonate. Incubation overnight at room temperature afforded 9 mg of the N-labeled product **BCK(N-fluorescence thiourea)PC** (**77**) (IC₅₀ = 10 nM after purification by preparative C₁₈ HPLC. The product **77** was characterized by HPLC and mass spectrometry as above and gave a negative ninhydrin test confirming that labeling occurred on the lysine side chain.

Peptide Mass Spectral Data, Peptide (calcd; found MH⁺): **1** (590.67; 591.2 MH⁺), **2** (634.22; 635.2 MH⁺), **3** (562.20; 563.0 MH⁺), **4** (816.41; 818.2 MH⁺), **5** (703.29; 704.2 MH⁺), **6** (737.28; 738.5 MH⁺), **7** (776.29; 776.5 MH⁺), **8** (753.27; 754.1 MH⁺), **9** (725.27; 726.2 MH⁺), **10** (668.73; 669.5 MH⁺), **11** (597.65; 598.2 MH⁺), **12** (767.29; 767.7 MH⁺), **13** (752.29; 753.2 MH⁺), **14** (766.30; 767.2 MH⁺), **15** (595.64; 596.5 MH⁺), **16** (639.69; 640.5 MH⁺), **17** (611.68; 612.4 MH⁺), **18** (625.20; 626.0 MH⁺), **19** (645.21; 646.2 MH⁺), **20** (595.19; 596.0 MH⁺), **21** (555.16; 556.2 MH⁺), **22** (569.18; 570.0 MH⁺), **23** (609.71; 610.2 MH⁺), **24** (631.71; 632.2 MH⁺), **25** (553.65; 554.2 MH⁺), **26** (569.21; 570.2 MH⁺), **27** (569.21; 570.2 MH⁺), **28** (603.20; 604.0 MH⁺), **29** (607.13; 608.2 MH⁺), **30** (569.17; 570.2 MH⁺), **31** (659.23; 660.2 MH⁺), **32** (595.17; 596.2 MH⁺), **33** (581.32; 582.0 MH⁺), **34** (616.72; 617.5 MH⁺), **35** (589.23; 590.2 MH⁺), **36** (782.88; 783.2 MH⁺), **37** (781.91; 782.5 MH⁺), **38** (504.29; 505.2 MH⁺), **39** (503.31; 504.5 MH⁺), **40** (594.19; 595.2 MH⁺), **41** (569.18; 570.0 MH⁺), **42** (553.18; 554.2 MH⁺), **43** (510.21; 511.0 MH⁺), **44** (517.12; 518.0 MH⁺), **45** (555.12; 556.0 MH⁺), **46** (599.31; 600.2 MH⁺), **47** (575.11; 576.0 MH⁺), **48** (575.11; 576.0 MH⁺), **49** (569.18; 570.2 MH⁺), **50** (695.07; 696.0 MH⁺), **51** (587.11; 588.0 MH⁺), **52** (603.11; 604.0 MH⁺), **53** (602.67; 603.5 MH⁺), **54** (641.11; 642.0 MH⁺), **55** (578.11; 579.2 MH⁺), **56** (631.11; 632.2 MH⁺), **57** (637.11; 638.2 MH⁺), **58** (637.11; 638.2 MH⁺), **59** (553.64; 554.5 MH⁺), **60** (442.50; 443.5 MH⁺), **61** (456.13; 457.2 MH⁺), **62** (456.13; 457.2 MH⁺), **63** (470.21; 470.8 MH⁺), **64** (470.21; 471.0 MH⁺), **65** (496.51; 497.5 MH⁺), **66** (510.51; 511.5 MH⁺), **67** (504.29; 505.2 MH⁺), **68** (504.29; 505.2 MH⁺), **69** (518.59; 519.2 MH⁺), **70** (518.59; 519.2 MH⁺), **71** (524.09; 525.0 MH⁺), **72** (510.28; 511.2 MH⁺), **73** (524.28; 525.2 MH⁺), **74** (651.11; 652.0 MH⁺), **75** (507.61; 508.5 MH⁺), **76** (678.82; 679.9 MH⁺), **77** (1068.19; 1069.3 MH⁺).

Receptor Binding ELISA. Inhibitor concentrations affording 50% inhibition (IC₅₀s) of α4β1 binding to VCAM-1 was determined by a protein-based receptor binding ELISA. The α4β1 was extracted from Ramos cell membranes using wheat germ lectin Sepharose chromatography followed by gel filtration in 1% octyl glucoside. MnCl₂ (1 mM) was included in all buffers during purification procedures and assays to maintain the active binding state. Recombinant soluble human VCAM-1 (55 kDa fragment composed of the first five N-terminal Ig-like domains) was purified from Chinese hamster ovary (CHO) cell culture media. Nunc Maxisorp 96-well plates were coated with 4 μg/mL VCAM-1 in phosphate-buffered saline. The wells were blocked with 1% bovine serum albumin in phosphate-buffered saline. Diluted samples of test inhibitor molecules were evaluated for blocking of α4β1 binding to VCAM-1 by addition of 50 μL of each inhibitor to the VCAM-1-coated wells prior to the addition of 50 μL of optimally diluted α4β1. The assay buffer was composed of 50 mM Tris-HCl (pH 7.4), 100 mM NaCl, 1 mM MnCl₂, and 0.05% Tween-20. The sample and α4β1 were allowed to incubate in the wells for 2 h at 37 °C. The bound α4β1 was detected with a nonblocking mouse anti-human β1 integrin monoclonal antibody (clone 2D4.6; Genentech, Inc.) followed by goat anti-mouse horseradish peroxidase (BioSource International, Camarillo, CA). Peroxidase activity was detected with TMB microwell peroxidase substrate (Kirkegaard and Perry Laboratories, Inc., Gaithersburg, MD). Reactions were stopped with 1 M phosphoric acid, and absorbance was measured at 450 nm. Results were plotted as absorbance vs concentration, and the concentration of peptide at the half-maximal absorbance value is reported as the IC₅₀.

Cell Adhesion Binding Assays. As a secondary assay, the ability of test molecules to inhibit binding of Ramos cells (American Type Culture Collection, Bethesda, MD) to VCAM-1 was assessed. Ramos cells were labeled with calcein (Molecular Probes, Eugene, OR). Nunc Maxisorp 96-well plates were coated with 2 μg/mL rabbit anti-human IgG (Fc specific;

Jackson Immunoresearch Laboratories, West Grove, PA). The wells were blocked with 1% bovine serum albumin in phosphate-buffered saline. Human VCAM-1-IgG chimera (domains 1 and 2 of human VCAM-1 linked to the CH₂ and CH₃ regions of human IgG1) was captured onto the anti-IgG-coated surfaces during a 1 h incubation. Diluted test compounds (10 μ L) were added to 40 μ L of binding buffer (4 mM CaCl₂, 4 mM MgCl₂ in 50 mM Tris-HCl, pH 7.5) in the washed assay wells. This was followed by 2×10^5 cells in 50 μ L of 1% bovine serum albumin in phosphate-buffered saline. Cells were allowed to bind for 1 h at room temperature. Unbound cells were removed by gentle washing. Bound cells were lysed with 1% SDS in Tris-HCl at pH 8.0. The fluorescence was recorded on a Cytofluor 2350 plate reader (Millipore, Bedford, MA) with filters set at 485 nm excitation and 530 nm emission.

NMR Structural Analysis. Peptide **5** (3.5 mg) was dissolved in 500 μ L of 90% H₂O/10% D₂O/25 mM sodium acetate-d₃, pH 3.9. All NMR spectra were acquired at 7 °C on a Bruker AMX-500 spectrometer. In addition to a high-resolution one-dimensional ¹H NMR spectrum, the following homonuclear two-dimensional (2D) NMR spectra were recorded using standard pulse sequences and phase cycling: COSY, TOCSY, NOESY, and ROESY.⁴² All 2D spectra were acquired in the phase-sensitive mode using time-proportional phase incrementation for quadrature detection in the *t*₁ dimension.⁴³ The solvent signal was suppressed by low-power phase-locked presaturation for 1.5 s. The TOCSY spectrum was acquired using a 96 ms "clean" DIPSI-2rc isotropic mixing sequence.⁴⁴ The NOESY spectrum was acquired with irradiation of solvent during the 350 ms mixing time. The ROESY spectrum was acquired with a mixing time of 175 ms and a spin-lock field strength of 4 kHz. Spectra were processed and analyzed on Silicon Graphics workstations using the program FELIX (Biosym Technologies). Resonance assignments were obtained using standard methods utilizing the 2D spectra discussed above.⁴⁵

NOE cross-peaks were characterized according to their integrated volumes as strong, medium, or weak, corresponding to upper bound distance restraints of 2.7, 3.5, and 4.5 Å, respectively; pseudoatom corrections were added when necessary.⁴⁶ Dihedral angle restraints for ϕ and χ_1 and stereospecific resonance assignments for the β -methylenes of Asp4, Pro5, and Cys6 were derived from coupling constants measured from 1D spectra and ROE data. Distance geometry calculations were carried out using DGII (Biosym Technologies). Fifty structures were calculated, and the 30 with the lowest total restraint violations were further refined with restrained molecular dynamics and minimization using the program DISCOVER (Biosym Technologies). The all-atom AMBER force field^{47,48} was used with a 15.0 Å cutoff for nonbonded interactions and a distance-dependent dielectric constant ($\epsilon = 4r$) to compensate for the lack of explicit solvent. Side chain and terminal charges were reduced to give total charges of ± 0.2 in order to reduce artifacts due to charge-charge interactions.

Lymphocyte Homing Assay. The *in vivo* activity of inhibitor **17** was evaluated in a lymphocyte homing assay using 4×10^6 ⁵¹Cr-labeled syngeneic mesenteric lymph node cells administered to normal 6–8 week old female BALB/c mice (Jackson Laboratories, Bar Harbor, ME) according to a modified procedure described by Hamann *et al.*⁴¹ Cells were labeled with 150 μ Ci of ⁵¹Cr (Amersham, Arlington Heights, IL) for 25 min at 37 °C. Mice were injected intravenously with radiolabeled cells in the presence of 0.5 mg of test peptide at time 0. The animals were sacrificed 1 h after receiving the radiolabeled cells. The Peyer's patches and inguinal lymph nodes were collected and counted for accumulated radioactivity. The PS/2 monoclonal antibody against the $\alpha 4$ subunit (American Type Culture Collection) was used as a positive control at 0.67 μ M given intravenously at time 0. The number of lymph node cells based upon accumulated radioactivity in various tissues is reported.

Acknowledgment. We would like to thank our collaborators Jeff Tilley, Barry Wolitzky, Kuo-Sen Huang, and Shirley Li at Roche (Nutley, NJ) for their input on

this project and for supplying us with the human VCAM used in the protein assay.

References

- (1) Hynes, R. O. Integrins: versatility, modulation, and signaling in cell adhesion. *Cell* **1992**, *69*, 11–25.
- (2) Hemler, M. E. VLA proteins in the integrin family: structures, functions, and their role on leukocytes. *Annu. Rev. Immunol.* **1990**, *8*, 365–368.
- (3) Sharar, S. R.; Winn, R. K.; Harlan, J. M. The adhesion cascade and anti-adhesion therapy: an overview. *Springer Semin. Immunopathol.* **1995**, *16*, 359–378.
- (4) Nakajima, H.; Sano, H.; Nishimura, T.; Yoshida, S.; Iwamoto, I. Role of VCAM-1/VLA-4 and ICAM-1/LFA-1 interactions in antigen-induced eosinophil and T cell recruitment into the tissue. *J. Exp. Med.* **1994**, *179*, 1145–1154.
- (5) Butcher, E. C.; Picker, L. J. Lymphocyte homing and homeostasis. *Science* **1996**, *272*, 60–66.
- (6) Elices, M. J.; Osborn, L.; Takada, Y.; Crouse, C.; Luhowsky, S.; Hemler, M. E.; Lobb, R. R. VCAM-1 on activated endothelium interact with the leukocyte integrin VLA-4 at a site distinct from the VLA-4/fibronectin binding site. *Cell* **1990**, *60*, 577–584.
- (7) Makarem, R.; Newham, P.; Askari, J. A.; Green, L. J.; Clements, J.; Edwards, M.; Humphries, M. J.; Mould, A. P. Competitive binding of VCAM-1 and the HepII/IIIcS domain of fibronectin to the integrin $\alpha 4\beta 1$. *J. Biol. Chem.* **1994**, *269*, 4005–4011.
- (8) Chuluyan, H. E.; Issekutz, A. C. $\alpha 4$ Integrin-dependent emigration of monocytes. *Springer Semin. Immunopathol.* **1995**, *16*, 391–404.
- (9) Simmons, P. J.; Masinovsk, B.; Longenecker, B. M.; Berenson, R.; Torok-Storb, B.; Gallatin, W. M. VCAM-1 expressed by bone marrow stromal cells mediates the binding of hematopoietic progenitor cells. *Blood* **1992**, *80*, 388–395.
- (10) Juliano, R. L.; Varner, J. A. Adhesion molecules in cancer: the role of integrins. *Curr. Opin. Cell Biol.* **1993**, *5*, 812–818.
- (11) Laberge, S.; Rabb, H.; Issekutz, T. B.; Martin, J. G. Role of VLA-4 and LFA-1 in allergen-induced airway hyperresponsiveness and lung inflammation in the rat. *Am. J. Respir. Crit Care Med.* **1995**, *151*, 822–829.
- (12) Barbadillo, C.; G-Arroyo, A.; Salas, C.; Mulero, J.; Sanchez-Madrid, F.; Andreu, J. L. Anti-integrin immunotherapy in RA: protective effect of anti- $\alpha 4$ antibody in adjuvant arthritis. *Springer Semin. Immunopathol.* **1995**, *16*, 375–379.
- (13) Podalski, D. K. Inflammatory bowel disease. *N. Engl. J. Med.* **1991**, *325*, 928–937.
- (14) Powrie, F.; Leach, M. W. Genetic and spontaneous models of inflammatory bowel disease in rodents: evidence for abnormalities in mucosal immune regulation. *Ther. Immunol.* **1995**, *2*, 115–123.
- (15) Papayannopoulou, T.; Craddock, C.; Nakamoto, B.; Priestley, G. V.; Wolf, N. S. The VLA-4/VCAM-1 adhesion pathway defines contrasting mechanisms of lodgement of transplanted murine hemopoietic progenitors between bone marrow and spleen. *Proc. Natl. Acad. Sci. U.S.A.* **1995**, *92*, 9647–9651.
- (16) Papayannopoulou, T.; Nakamoto, B. Peripheralization of hemopoietic progenitors in primates treated with anti-VLA-4 integrin. *Proc. Natl. Acad. Sci. U.S.A.* **1993**, *90*, 9374–9378.
- (17) Barker, P. L.; Bullens, S.; Bunting, S.; Burdick, D. J.; Chan, K. S.; Deisher, T.; Eigenbrot, C.; Gadek, T. R.; Gantzios, R.; Lipari, M. T.; Muir, C. D.; Napier, M.; Pitti, R. M.; Padua, A.; Qian, C.; Stanley, M.; Struble, M.; Tom, J.; Burnier, J. P. Cyclic RGD peptide analogs as antiplatelet antithrombotics. *J. Med. Chem.* **1992**, *35*, 2040–2048.
- (18) McDowell, R. S.; Blackburn, B. K.; Gadek, T. R.; McGee, L. R.; Rawson, T.; Reynolds, M. E.; Robarge, K. D.; Somers, T. C.; Thorsett, E. D.; Tichler, M.; Webb, R.; Venuti, M. C. From peptide to non-peptide. The de novo design of potent, non-peptidic inhibitors of platelet aggregation based on a benzodiazepinedione scaffold. *J. Am. Chem. Soc.* **1994**, *116*, 5077–5083.
- (19) Nowlin, D. M.; Gorcsan, F.; Moscinski, M.; Chiang, S.; Lobl, T. J.; Cardarelli, P. M. A novel cyclic pentapeptide inhibits $\alpha 4\beta 1$ and $\alpha 5\beta 1$ integrin-mediated cell adhesion. *J. Biol. Chem.* **1993**, *268*, 20352–20359.
- (20) Kieffer, N.; Phillips, D. R. Platelet membrane glycoproteins: functions in cellular interactions. *Annu. Rev. Cell Biol.* **1990**, *6*, 329–357.
- (21) Pytela, R.; Pierschbacher, M. D.; Ruoslahti, E.; A 125/115-kDa cell surface receptor specific for vitronectin interacts with the RGD adhesion sequence derived from fibronectin. *Proc. Natl. Acad. Sci. U.S.A.* **1985**, *82*, 5766–5770.
- (22) Cardarelli, P. M.; Yamagata, S.; Taguchi, I.; Gorcsan, F.; Chiang, S.; Lobl, T. The collagen receptor $\alpha 2\beta 1$, from MG-63 and HT1080 cells, interacts with a cyclic RGD peptide. *J. Biol. Chem.* **1992**, *267*, 23159–23164.
- (23) Osborn, L.; Vassallo, C.; Benjamin, C. D. Activated endothelium binds lymphocytes through a novel binding site in the alternatively spliced domain of VCAM-1. *J. Exp. Med.* **1992**, *176*, 99–107.

- (24) Jones, E. Y.; Harlos, K.; Bottomley, M. J.; Robinson, R. C.; Driscoll, P. C.; Edwards, R. M.; Clements, J. M.; Dungeon, T. J.; Stuart, D. I. Crystal structure of an integrin-binding fragment of vascular cell adhesion molecule-1 at 1.8Å resolution. *Nature* **1995**, *373*, 539–544.
- (25) Wang, J.; Pepinsky, R. B.; Stehle, T.; Liu, J.; Karpusas, M.; Browning, B.; Osborn, L. The crystal structure of an N-terminal two-domain fragment of vascular cell adhesion molecule 1 (VCAM-1): a cyclic peptide based on the domain 1 C-D loop can inhibit VCAM-1- $\alpha 4\beta 1$ integrin interaction. *Proc. Natl. Acad. Sci. U.S.A.* **1995**, *92*, 5714–5718.
- (26) Renz, M. E.; Chiu, H. H.; Jones, S.; Fox, J.; Kim, K. J.; Presta, L. G.; Fong, S. Structural requirements for adhesion of soluble recombinant murine VCAM-1 to $\alpha 4\beta 1$. *J. Cell. Biol.* **1994**, *125*, 1395–1406.
- (27) Quan, C.; Skelton, N.; Clark, K.; Jackson, D. Y.; Renz, M. E.; Chiu, H. H.; Keating, S. M.; Beresini, M.; Fong, S.; Artis, D. R. Structure-based design of small, potent cyclic peptides which mimic the binding epitope of VCAM. Submitted for publication.
- (28) Chiu, H. H.; Crowe, D. T.; Renz, M. E.; Presta, L. G.; Jones, S.; Weismann, I. L.; Fong, S. Similar but nonidentical amino acid residues on VCAM-1 are involved in the interaction with $\alpha 4\beta 1$ and $\alpha 4\beta 7$ under different activity states. *J. Immunol.* **1995**, *155*, 5257–5267.
- (29) Pierschbacher, M. D.; Ruoslahti, E. Influence of stereochemistry of the sequence Arg-Gly-Asp-Xaa on binding specificity in cell adhesion. *J. Biol. Chem.* **1987**, *262*, 17294–17298.
- (30) Lobl, T. J.; Chiang, S.; Cardarelli, P. M. Cyclic cell adhesion modulation compounds. World Patent 92/00995, 1992.
- (31) Komoriya, A.; Green, L. J.; Mervic, M.; Yamada, S. S.; Yamada, K. M.; Humphries, M. J. The minimal essential sequence for a major cell type-specific adhesion site (CS1) within the alternatively spliced type III connecting segment domain of fibronectin is leucine-aspartic acid-valine. *J. Biol. Chem.* **1991**, *266*, 15075–15079.
- (32) Chung, J. Y. L.; Wasicak, J. T.; Arnold, W. A.; May, C. S.; Nadzan, A. M.; Holiday, M. W. Conformationally constrained amino acids. Synthesis and optical resolution of 3-substituted proline derivatives. *J. Org. Chem.* **1990**, *55*, 270–275.
- (33) Viney, J. L.; Jones, S.; Chiu, H. H.; Lagrimas, B.; Renz, M. E.; Presta, L. G.; Jackson, D. Y.; Hillan, K. J.; Lew, S.; Fong, S. Mucosal addressin cell adhesion molecule 1: a structural and functional analysis demarcates the integrin binding motif. *J. Immunol.* **1996**, *157*, 2488–2497.
- (34) Koivunen, E.; Gay, D. A.; Ruoslahti, E. Selection of peptides binding to the $\alpha 5\beta 1$ integrin from phage display library. *J. Biol. Chem.* **1993**, *266*, 20205–20210.
- (35) Holzmann, B.; Weismann, I. L. Peyer's patch-specific lymphocyte homing receptors consist of a VLA-4-like α chain associated with either of two integrin β chains, one of which is novel. *EMBO* **1989**, *8*, 1735–1741.
- (36) Holzmann, B.; McIntyre, B. W.; Weismann, I. L. Identification of a murine Peyer's patch-specific lymphocyte homing receptor as an integrin molecule with an α chain homologous to human VLA-4 α . *Cell* **1989**, *56*, 37–46.
- (37) Pasqualini, R.; Bourdoulous, S.; Koivunen, E., Jr.; Ruoslahti, E. A polymeric form of fibronectin has antimetastatic effects against multiple tumor types. *Nature Medicine* **1996**, *2*, 1197–1203.
- (38) Merrifield, R. B. Solid phase peptide synthesis 1. The synthesis of a tetrapeptide. *J. Am. Chem. Soc.* **1963**, *85*, 2149–2154.
- (39) Carpino, L. A.; Han, G. Y.; Fluorenylmethyl carbamate protection for amino acids. *J. Org. Chem.* **1972**, *37*, 3404–3409.
- (40) Wang, S. S.; Kulesha, I. D.; Winter, D. P.; Makofske, R.; Kutney, R.; Meinhofer, J. Preparation of protected peptide hydrazides from the acids and hydrazine by dicyclohexylcarbodiimide-hydroxybenzotriazole coupling. *Int. J. Pept. Protein Res.* **1978**, *11* (4), 297–299.
- (41) Hamann, A.; Andrew, D. P.; Jablonski-Westrich, D.; Holzmann, B.; Butcher, E. C. Role of $\alpha 4$ -integrins in lymphocyte homing to mucosal tissues in vivo. *J. Immunol.* **1994**, *152*, 3282–3285.
- (42) Cavanagh, J.; Fairbrother, W. J.; Palmer, A. G.; Skelton, N. J. *Protein NMR Spectroscopy: Principles and Practice*; Academic Press: San Diego, CA, 1995.
- (43) Marion, D.; Wuthrich, K. Application of phase sensitive two-dimensional correlated spectroscopy (COSY) for measuring ^1H - ^1H spin-spin coupling constants in proteins. *Biochem. Biophys. Res. Commun.* **1983**, *113*, 967–974.
- (44) Cavanagh, J.; Rance, M. Suppression of cross-relaxation effects in TOCSY spectra via a modified DIPSI-2 mixing sequence. *J. Magn. Reson.* **1992**, *96*, 670–678.
- (45) Wuthrich, K. *NMR of Proteins and Nucleic Acids*; John Wiley & Sons, Inc.: New York, 1986.
- (46) Wuthrich, K.; Billeter, M.; Braun, W. Pseudostructures for the 20 common amino acids for use in studies of protein conformation by measurements of intramolecular proton-proton distance constraints with nuclear magnetic resonance. *J. Mol. Biol.* **1983**, *169*, 949–961.
- (47) Weiner, S. J.; Kollman, P. A.; Case, D. A.; Singh, U. C.; Ghio, C.; Alagona, G. S.; Profeta, J.; Weiner, P. A new force field for molecular mechanical simulation of nucleic acids and proteins. *J. Am. Chem. Soc.* **1984**, *106*, 765–784.
- (48) Weiner, S. J.; Kollman, P. A.; Nguyen, D. T.; Case, D. A. An all-atom force field for simulations of proteins and nucleic acids. *J. Comput. Chem.* **1986**, *7*, 230–252.

JM970175S